CORROSION SCIENCE AND TECHNOLOGY, Vol.2, No.6(2003), pp.289~295

A Study on Corrosion Resistance Characteristics of PVD Cr-N Coated Steels by Electrochemical Method

SeungHo Ahn, JiHong Yoo, YoonSeok Choi, JungGu Kim, and JeonGun Han

Department of Advanced Materials Engineering, Sung Kyun Kwan University
300, Chunchun-Dong, Jangan-Gu, Suwon, 440-746, KOREA

The corrosion behavior of Cr-N coated steels with different phases (α-Cr, CrN and Cr_2N) deposited by cathodic arc deposition on H13 steel was investigated in 3.5% NaCl solution at ambient temperature. Potentiodynamic polarization test, electrochemical impedance spectroscopy (EIS) and scanning electron microscopy (SEM) were the techniques applied to characterize the corrosion behavior. It was found that the CrN coating had a lower current density from potentiodynamic polarization test than others. The porosity, corresponding to the ratio of the polarization resistance of the uncoated and the coated substrate, was higher in the Cr_2N coating than in the other Cr-N coated steels. EIS measurements showed, for the most of Cr-N coated steels, that the Bode plot presented two time constants. Also, the Cr_2N coating represents the characteristic of Warburg behavior after 72hr of immersion. The coating morphologies were examined in planar view and cross-section by SEM analyses and the results were compared with those of the electrochemical measurement. The CrN coating had a dense, columnar grain-sized microstructure with minor intergranular porosity. From the above results, the CrN coating provided a better corrosion protection than the other Cr-N coated steels.

Keywords : *cathodic arc deposition, potentiodynamic polarization test, electrochemical impedance spectroscopy, warburg behavior, porosity*

1. Introduction

Electrochemical hard chromium coatings have been used in many technical applications for many decades. However, because of environmental concerns, there have been some efforts for several years to replace electroplated chromium by other deposition methods with fewer environmental problems. Thus, the development of clean technologies in all spheres of industrial manufacturing is an essential task, not only for material and metal finishing but also for plasma surface engineering. Nitride-based hard coatings have proven their capability in increasing tool lifetime when being exposed to abrasive and corrosive environments. Within the aim of this, Cr-N hard coatings were deposited on steel substrate by cathodic arc deposition. Cr-N coated steels produced by the cathodic arc deposition process have many advantages, such as fine-grained structure, low internal stress, excellent adhesion, chemical inertness and good thermal stability up to 700℃.[1] Cathodic arc deposition is one of the most suitable technologies for depositing hard coatings, due to its characteristics including nearly fully ionized plasma and high energy of ions.[2] The Cr-N coatings were formed different phases under different nitrogen partial pressure, such as α - Cr, CrN and Cr_2N.[3] There were some investigations about the corrosion characteristics of Cr-N coatings[4),5)] However, little information exists on their corrosion characteristics with different phases.

The aim of this paper is to evaluate the corrosion protection of steel substrates by Cr-N hard coatings with different phases performed by reactive cathodic arc evaporation. The corrosion characteristics of these materials were investigated by potentiodynamic polarization test, electrochemical impedance spectroscopy (EIS) in a 3.5% NaCl solution at room temperature.

In the present paper, electrochemical behaviors were outlined. The effects of porosity were discussed. Finally, optimized conditions were given for the improvement of corrosion resistance by cathodic arc deposition process.

2. Experimental

2.1 Material preparation and coating deposition

The chemical composition of the hot working tool steel (H13) is listed in Table 1. Samples having 25×25 mm were cut from the 5 mm thick sheet, mechanically polished using 2000 grit SiC for the final step. The samples were rinsed with acetone and submitted an ultrasonic washing

Table 1. Chemical compositon of H13 in wt.%.

Element	C	Mo	Cr	V	Si	Mn	P	S	Fe
wt.%	0.37	1.3	5.0	1.0	1.0	0.5	0.03	0.03	Bal.

Table 2. Main deposition conditions

Bias voltage	-200 V
Residual pressure	1×10^{-5} Torr
Nitrogen working pressure	1×10^{-4}, 2×10^{-2}, 1×10^{-3} Torr
Temperature	200℃
Cathodic current	50 A
Depositon time	1 ~ 2 hr
Thickness	3.2 ㎛

in acetone for 5min. The coatings were deposited by evaporated pure Cr solid cathode in a nitrogen atmosphere (1×10^{-4} ~ 1×10^{-3} Torr). The substrate was biased up to -200V. The chamber was evacuated to a pressure of 1×10^{-5} Torr. The deposition temperature (200℃) was maintained by using radiant heaters. The film thickness was approximately 3.2 ㎛. The major deposition parameters used in this study are summarized in Table 2.

A 3.5% NaCl solution, prepared with analytical grade reagents and deionized water, was used to simulate the saline environments. The working surface was partially masked with nonreactive paint to avoid crevice corrosion attack. The exposed surface area was 0.64 cm^2. To have a better statistical basis for analysis, three samples were generated per coating condition.

2.2 Corrosion testing

A conventional three-electrode cell was used with the counter electrode and a saturated calomel electrode (SCE) as a reference electrode. All electrochemical experiments were performed under exclusion of oxygen in 3.5% NaCl solution at room temperature. Degassing of the electrolyte was achieved by bubbling nitrogen through the solution. Potentiodynamic and EIS measurements have been obtained using an EG&G PAR 273A and EG&G Model 1025 frequency response analyzer with a computerized system for collection and analysis of the electrochemical data. Prior to the beginning of the polarization or EIS procedures, the specimens were kept in the solution for 1hr in order to establish the free corrosion potential(E_{corr}). Potentiodynamic polarization tests were obtained with a scan rate of 0.166 mV/s from the initial potential of -250 mV vs corrosion potential to the final potential of 400 mV_{SCE}. The measurement of the EIS spectra was recorded in the 1 mHz to 100 kHz frequency range, with a data density of five frequency points per decade. Sinusoidal voltage of ±5 mV was supplied and DC potential was set to E_{corr}. The impedance curves were fit to the coating model using the 'Zview' software and the characteristic coating parameters were determined.

2.3 Porosity measurement

The film coatings produced by physical vapor deposition methods often exhibit porosity. This porosity can weaken the interfacial material and provide an easy fracture path for adhesion failure. Local defects can form a direct path between the corrosive environment and the substrate and the risk of galvanic corrosion also exists.[6] By using electrochemical techniques, it is possible to estimate the porosity of these coatings. The porosity can be determined from the measured polarization resistance. The polarization resistance can be experimentally determined from dc polarization curve.

3. Results

3.1 Characterization of films

The crystal structure was measured by X-ray diffraction (XRD) using Cu K_α radiation. To optimize the properties of the Cr-N coated steels, the effect of the nitrogen flow rate on the structure, phase and chemical composition was investigated. Experiments were carried out by the nitrogen partial pressure in the range of 5×10^{-5} Torr to 2×10^{-2} Torr. Fig. 1 shows XRD patterns of films as a function of various nitrogen partial pressure. In the lower nitrogen partial pressure range (5×10^{-5} ~ 1×10^{-4} Torr), the coating in this case exhibits single-phase BCC structure with predominant Cr(110) and Cr(200) crystallographic orientations. In the range of 8×10^{-4} Torr to 1×10^{-2} Torr, a mixture of Cr_2N(111) and CrN ((111), (200) and (220)) phases has been identified. In the highest nitrogen partial pressure (2×10^{-2} Torr), the coating exhibits a NaCl unit

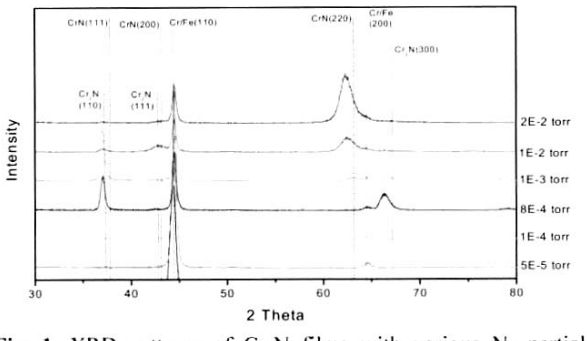

Fig. 1. XRD patterns of Cr-N films with various N_2 partial pressure

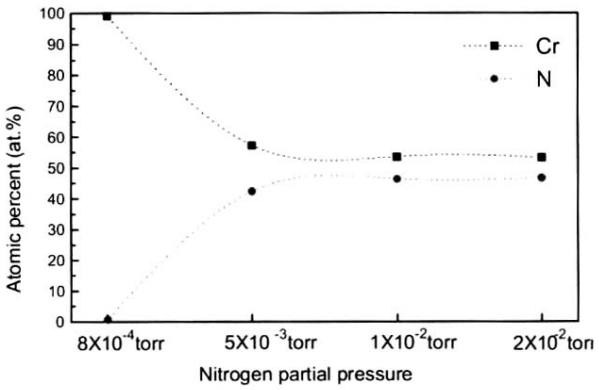

Fig. 2. Variation of Cr : N at.% for Cr-N films with various N_2 partial pressure

cell structure and a strong CrN(220) texture.[3]

AES investigation was performed to determine the influence of the nitrogen partial pressure on the chemical composition of the Cr-N hard coatings. When the nitrogen partial pressure higher than 1×10^{-2} Torr was introduced into the vacuum chamber, the Cr-N coatings with stoichiometric (Cr : N = 1.17) composition were achieved, as shown in Fig. 2.

From above results, depending on the chemical composition of the coatings, the cubic chromium, hexagonal Cr_2N (a=4.759 Å, c=4.438 Å) and cubic CrN (a=4.149 Å) phases could be detected. These results agree very well with the Cr-N phase diagram.[7]

The planar and cross sectional morphologies of the Cr-N coated steels are shown in Fig. 3. The coating contained droplet growth defects of various sizes and of non-uniform distribution, visible from the surface and in cross section. The droplets were poorly bonded to the film and they easily came out, leaving a pinhole in the film. The CrN coating had a dense, columnar grain-sized microstructure with minor intergranular porosity and pinholes. The contrast between the droplets and the coatings was not only different, suggesting their different chemical composition, but also to a different extent suggesting certain variations in the composition of each individual droplet.[4]

3.2 Potentiodynamic corrosion measurements

The evolutions of the potentiodynamic polarization measurements of the Cr-N coated steels are shown in Fig. 4. The anodic poarization curves of Cr-N coated steels reproduced some features of the substrate in shape. The coated steels had more noble potentials of -581.5 mV_{SCE} ~ -556.7 mV_{SCE} as compared with -726 mV_{SCE} for the uncoated steel. The result also indicated that the corrosion current density of CrN was lower (< 0.5359 $\mu A/cm^2$) than others, so that the CrN coating had better corrosion resistance than others.

The corrosion appearance is closely related to the coated surface quality, e.g., coated surface morphology and defects (pinhole, porosity and so on). This directly influences the corrosion resistance of coatings. This indicates that the electrolyte has reached the substrate through micropores in the coating and caused its dissolution. Porosity corresponds simply to the ratio of the polarization resistance of the uncoated and the coated substrate.

$$P = \frac{R_{p,u}}{R_{p,r\text{-}u}}$$

where P is the total coating porosity, $R_{p,u}$ is the polarization resistance of the substrate and $R_{p,r\text{-}u}$ is the measured polarization resistance of coating-substrate system.[8] Combining the equation of W. Tato et al. with the electrochemical determinations gives a porosity rate of 0.0041% for Cr_2N, 0.0015% for CrN, and of only 0.0003% for α-Cr listed in Table 3. The porosity is somewhat higher in the Cr_2N coating than in the other Cr-N coated steels. These results are in agreement with the SEM observations of Cr-N coated steels in Fig. 3.

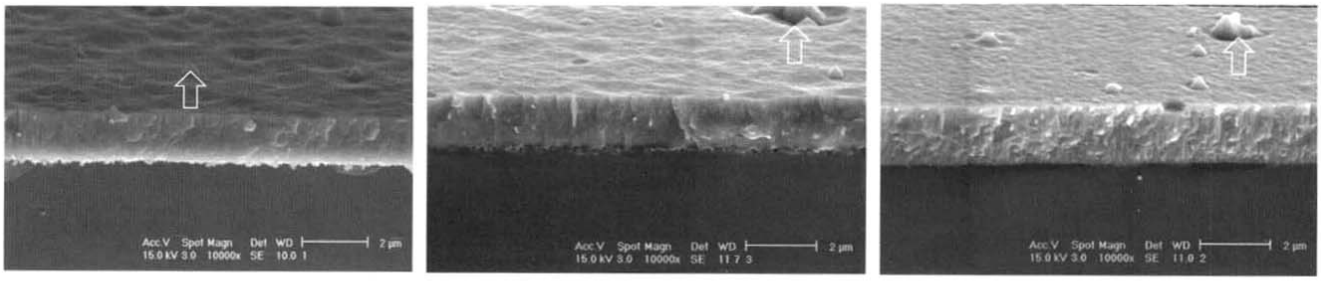

(a) α-Cr (b) CrN (c) Cr_2N

Fig. 3. Scanning electron micrographs of cross-section (⇧: droplet)

Table 3. Porosity of PVD coatings on H13 from DC polarization data

Specimen	E_{corr} (m V)	i_{corr} (μA/㎠)	$R_{p,u}$ (Ω ㎠)	$R_{p,r-u}$ (Ω ㎠)	Calculated porosity (%)
α-Cr	-581.5	0.0392	2.91322	759.79×10^{3}	0.0003
CrN	-556.7	0.2034	2.91322	188.48×10^{3}	0.0015
Cr_2N	-558.2	0.5359	2.91322	70.344×10^{3}	0.0041

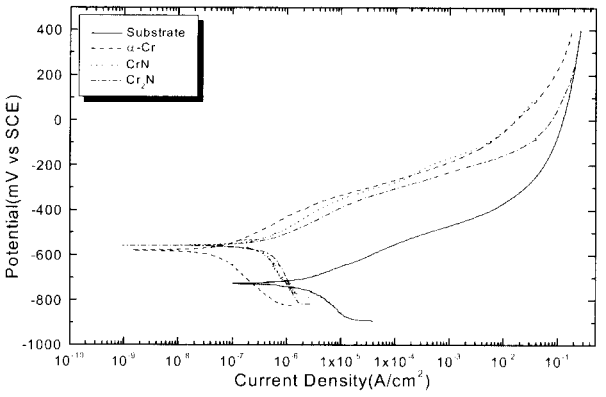

Fig. 4. Potentiodynamic polarization curves

3.3 Impedance measurements

EIS data were displayed as Bode plots (Log[Z] vs Log(Freq) and Phase angle vs Log(Freq)). This Bode plots of the Cr-N coated steels immersed for different periods are shown in Fig. 5. These data show typically two time constants which were better resolved at the longer exposure times. This effect was accompanied by a continuous and slight decrease in the absolute values of the impedance, more noticeable in the low frequency limit of the spectra. The equivalent circuit represented in Fig. 6 was applied to model the EIS data for coatings, and enabled the parameter values for the individual elements to be determined with a least squares analysis. The equivalent circuit consists of the following elements : a solution resistance R_s of the test electrolyte between the working electrode and the reference electrode, a capacitance C_{pore} and a charge transfer resistance R_{ct} for defects in the coatings, and a capacitance C_{coat} and a charge transfer resistance R_{pore} for the porosity resistance of coating layer. The explanation for a charge transfer resistance R_{ct} comes from the penetration of the electrolyte through the pores or pinholes existing in the coating.[9),10)] The optimized values for the various parameters are given in Table 4 for the α-Cr, CrN and Cr_2N coated specimens, respectively. Constant-phase elements (CPEs) are widely

Table 4. Electrochemical parameters obtained by equivalent circuit simulation

Exposure time		R_s (Ω ㎠)	CPE1		R_{coat} (Ω ㎠)	CPE2		R_{ct} (Ω ㎠) *W-R	* * WSS
			C_{coat} (F/㎠)	n (0-1)		C_{pore} (F/㎠) *W-Q	n (0-1)		
Substrate		0.6069	2.2897×10^{-3}	0.639	217.1	96.55	0.510	2076	0.9
1 hr	α-Cr	1.313	4.0432×10^{-5}	0.952	287.9	3.9553×10^{-5}	0.765	18835	0.099
	CrN	0.3964	5.6628×10^{-5}	0.991	81.48	9.5831×10^{-5}	0.813	9704	0.034
	Cr_2N	0.251	4.775×10^{-5}	0.994	113.1	8.2879×10^{-5}	0.768	17449	0.029
24 hr	α-Cr	0.865	4.899×10^{-5}	0.955	136.5	1.7666×10^{-4}	0.791	11477	0.088
	CrN	0.7098	2.3498×10^{-4}	0.825	117.4	3.2413×10^{-4}	0.828	2490	0.03
	Cr_2N	0.1042	6.384×10^{-5}	0.976	91.71	5.8054×10^{-4}	0.725	5778	0.194
48 hr	α-Cr	0.6619	9.6352×10^{-5}	0.890	66.63	3.652×10^{-4}	0.901	3718	0.05
	CrN	0.6227	1.2029×10^{-4}	0.916	53.34	7.5256×10^{-4}	0.796	6846	0.173
	Cr_2N	0.2095	1.6338×10^{-4}	0.878	123.6	1.3504×10^{-3}	0.734	4242	0.193
72 hr	α-Cr	0.8061	1.0934×10^{-4}	0.890	27.93	1.2120×10^{-3}	0.893	3081	0.122
	CrN	0.5148	1.1075×10^{-4}	0.940	32.35	1.4338×10^{-3}	0.793	5353	0.249
	Cr_2N	0.0523	1.4084×10^{-4}	0.964	12.86	3.3112×10^{-1}	0.515	137.5	0.03

* : Warburg behavior (Substrate : after immersion 1hr, Cr_2N : : after immersion 72hr)
** : Weighted sum of squares

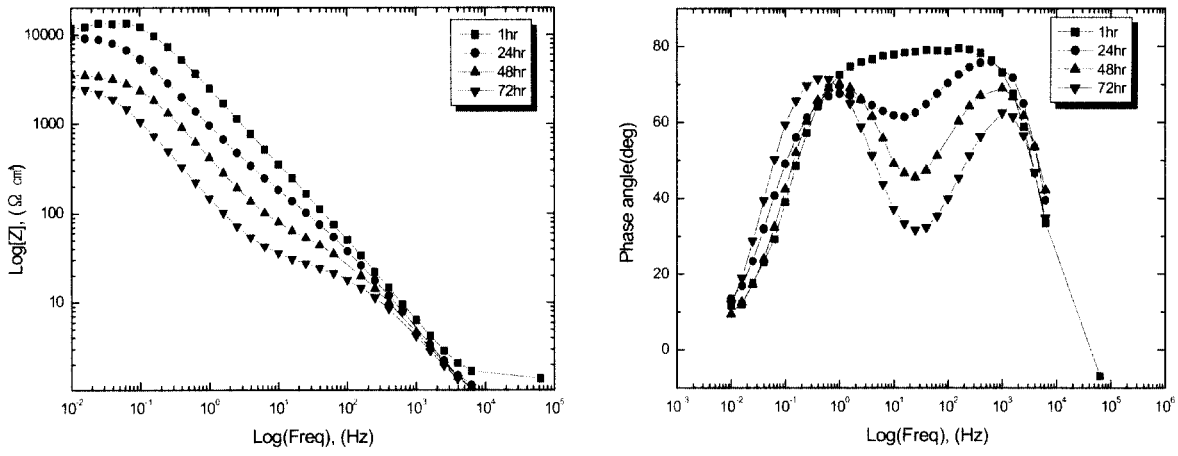

(a) α-Cr

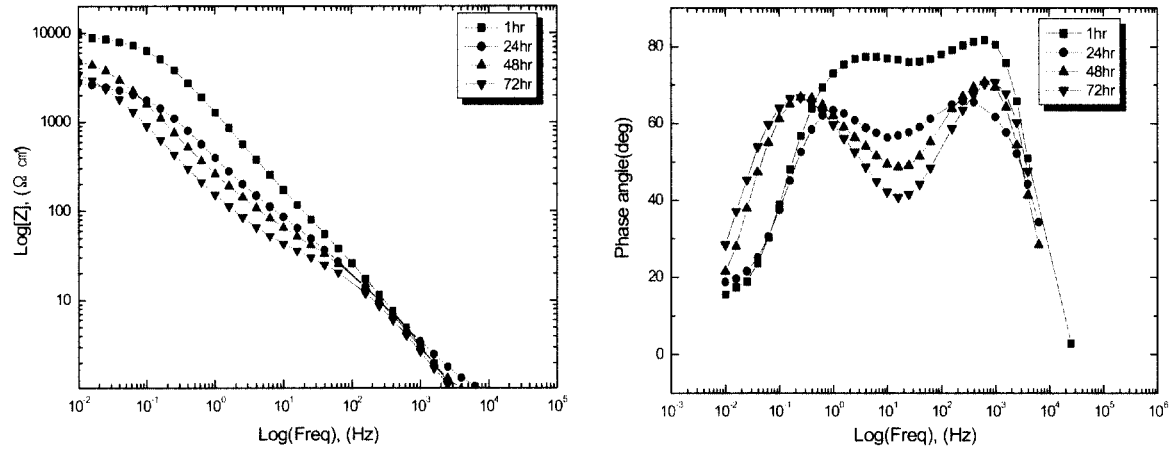

(b) CrN

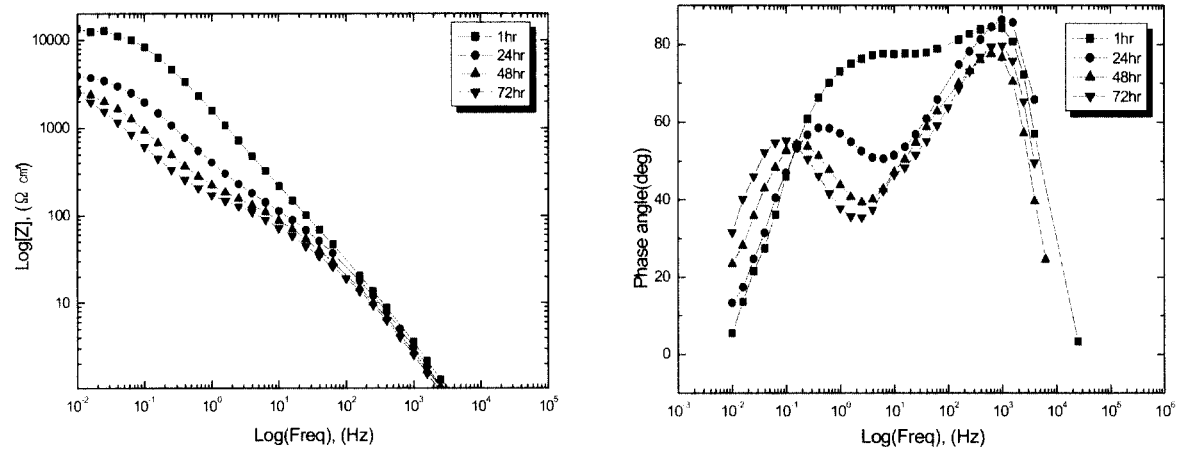

(c) Cr_2N

Fig. 5. Bode plots for EIS data of Cr-N coated steels for different exposure times

used in data fitting to allow for depressed semicircles. The capacitance is replaced with a CPE for better fit quality. A CPE accounts for deviations from ideal dielectric behavior related to surface inhomogeneity.

The impedance of CPE may be defined by, $Z_{CPE} = Z_0(j\omega)^n$

where Z_0 is the adjustable parameter used in the non-linear least squares fitting and the factor n, defined as a CPE power, is an adjustable parameter that always lies between 0.5 and 1. It can be obtained from the slope of [Z] on the Bode plot. When $n = 0.5$ the CPE represents a Warburg impedance with diffusional character. The low n values obtained for the coated samples should also be noticed, which indicated a rough surface of the coating film.[10),11)]

The initial coating capacitance C_{coat} was the highest for CrN, whereas the coating capacitance of CrN decreased during exposure for 72hr. For the α-Cr and the Cr_2N coatings, they showed much higher relative variations in resistance and capacitance compared to the CrN coating, which implies that the α-Cr and the Cr_2N coatings are more porous and less dense. The charge transfer resistance of the surface layer was shown in Fig. 7. Despite some differences at the initial exposure stage, the CrN presents higher R_{ct} values than others after 48hr. Thus, the CrN coating showed excellent performance during immersion in saline solution for 72hr, while for the other coatings significant degradation and loss of corrosion protection occurred.

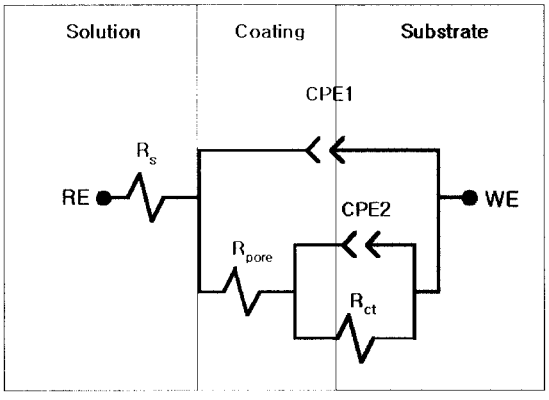

(a) for a pitted electrode

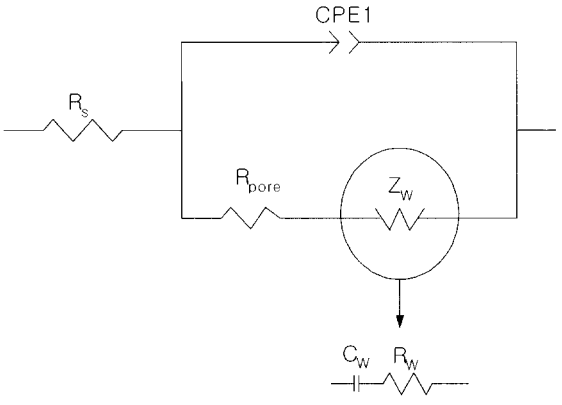

(b) for the interfacial impedance with a diffusion impedance

Fig. 6. Equivalent circuits to fit the electrochemical impedance spectroscopy diagram

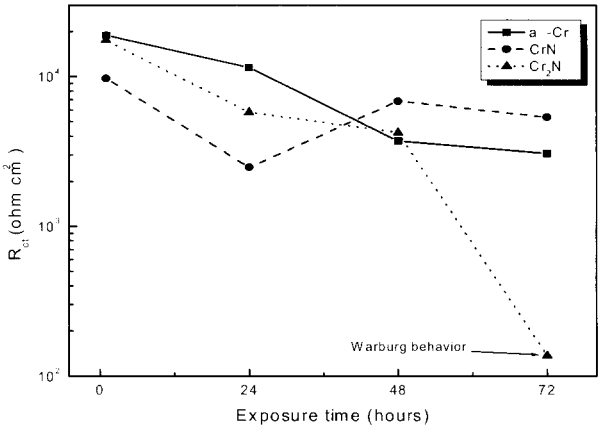

Fig. 7. Calculated charge transfer resistance for the α-Cr, CrN and Cr_2N coatings as a function of the exposure time.

For the comparison, the EIS spectrum of the uncoated sample after 1hr immersion in the test electrolyte was also recorded and is given in Fig. 8. Fig. 8(a) shows the result of the experimental and fitted data as Nyquist plot. In this case, the absolute impedance was about one order of magnitude smaller than in the case of the coated samples. Though the equivalent circuit in Fig. 6 could also be employed for the analysis of this impedance spectrum, the elements R_{pore} and C_{coat} described the electrochemical characteristics of the oxide layer on the surface of the metallic material instead.[12)] For the uncoated steel, the charge transfer resistance Rct was approximately 2×10^3 Ωcm^2, a result that indicated the dissolution of the metallic material in the electrolyte solution. These observations confirm the trends of polarization experiments. In addition, a Warburg diffusion phenomenon, which suggests a diffusion-controlled mechanism in the corrosion reaction, was observed in the low frequency region for immersion time of 1hr.

Also, the Cr_2N coating presents the same phenomenon as the uncoated steel after immersion time of 72hr. The accumulation of corrosion products in the pores of coatings generally favors the appearance of diffusion tails due to the concentration gradient between the corrosion product

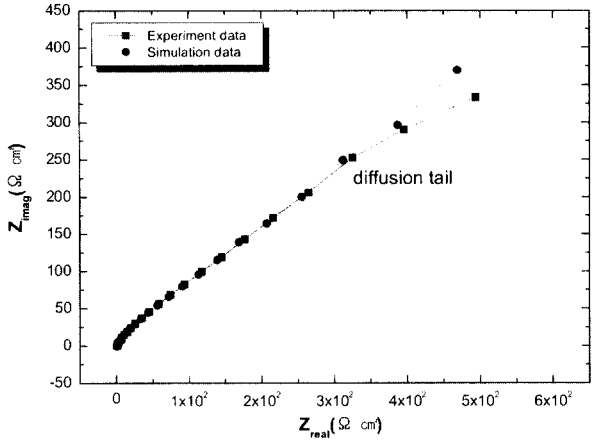

(a) Nyquist plot (experiment and simulation data)

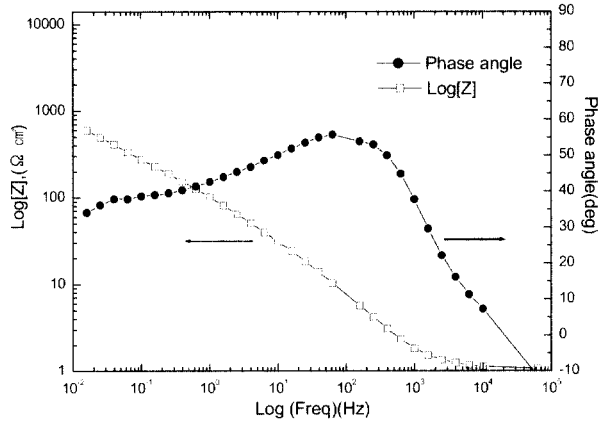

(b) Bode plot

Fig. 8. Experimental impedance diagrams of substrate (H13) after 1hour immersion.

and the bottom of pore. This caused the mass-transfer reaction. Thus, the substrate in the pore was heavily corroded as compared to the outer coating surface, and led to a rate-determining steps. An alternative equivalent circuit is proposed in which Z_W is represented by a series combination of a Warburg pseudoresistance(R_W) and a Warburg pseudocapacitance(C_W), shown in Fig. 6(b) previously.[13]

4. Conclusions

1) Analyzing the polarization curves, all the coated samples present a better corrosion resistance regarding the uncoated substrate. As the immersion time increases, the polarization resistance of Cr_2N coating is significantly decreased.

2) At the applied frequency range, the equivalent circuit employed for the description of the EIS spectra for the Cr-N coated steels provides the best fit of the experimental data. The low frequency parameters obtained from EIS data can be associated with the coating layer, and their variations show that the change in the localized corrosion behavior is at least partially associated with an increase of film porosity, resulting in a decrease of its resistance. The Cr_2N coating indicated that the porosity resistance R_{pore} and the charge transfer resistance R_{ct} significantly decreased with increasing degradation of the protective properties of the coating.

3) The CrN coating showed better behavior in saline environment. This better performance was due to the dense microstructure and the low porosity. The calculated porosity is roughly in agreement with the observed microstructure and polarization resistance.

References

1. S. S. Kim *Thin Solid Films*, **334**, 133 (1998).
2. D. M. Sanders, D. B. Boercker, and S. Falabella, *IEEE Trans. Plasma Sci.*, **18**(6), 474 (1990) .
3. T. B. Massalski, Binary Alloys Phase Diagrams, ASM Metals Park, 1 (1986).
4. H. W. Wang *Surface and Coating Technology*, **126**, 279 (2000).
5. M. Tomlinson *Vacuum*, **53**, 117 (1999).
6. J. Aromaa *Materials Science and Engineering*, **A140**, 722 (1991).
7. W. Herr, B. Matthes, and E. Broszeit, *Surface and coatings technology*, **60**, 428 (1993).
8. W. Tato and D. Landolt, *J. Electrochem. Soc.*, **145**, 4173 (1998).
9. R. M. Souto and H. Alanyali, *Corrosion Science*, **42**, 2201 (2000).
10. Gordon P. Bierwagen, L. He, J. Li, L. Ellingson, and D.E. Tallman, *Progress in Organic Coatings*, **39**, 67 (2000).
11. Bary C. Syrett, Electrochemical Impedance and Noise, NACE, 45 (1999).
12. G. Bellanger and J. J. Rameau, *Electrochim. Acta*, **40**, 2519 (1995).
13. S. R. Taylor and E. Gileadi, *Corrosion Science*, **51**, 64 (1995).